Granular Matter (2010) 12:107–123
DOI 10.1007/s10035-009-0158-y

Investigation of adequacy of multi-sphere approximation of elliptical particles for DEM simulations

D. Markauskas · R. Kačianauskas · A. Džiugys · R. Navakas

Received: 20 February 2009 / Published online: 9 December 2009

Abstract Adequacy of approximation of ellipsoidal particles composed of a set of sub-spheres for numerical Discrete Element Method (DEM) simulations is examined. The algorithm of adaptive hierarchical multi-sphere (MS) model is suggested for composing elliptical particles. Numerical simulation of the piling problem is used as a test problem for evaluating the adequacy of MS model approximation in comparison to the model of smooth ellipses for multiparticle system. The accuracy of MS approximation with the increasing number of sub-spheres is examined in detail by comparison of macroscopic and microscopic parameters of granular dynamics. It was determined that the data on macroscopic parameters yielded by the MS model tend to converge to those of the smooth ellipsoid with the increasing number of the constituent sub-spheres, and the MS model approximates the smooth perfect ellipsoid with a reasonable number of sub-spheres within the limits of the appropriate tolerance. It can be concluded that a multi-sphere model remains a realistic and relatively simple particle model applicable to DEM simulations of the behaviour of the real smooth and rough elliptically shaped particles.

Keywords Discrete element method · Elliptical shape · Multi-sphere approach · Composite particles · Piling · Numerical simulation

D. Markauskas · R. Kačianauskas
Laboratory of Numerical Modelling, Vilnius Gediminas Technical University, Saulėtekio al. 11, 10223 Vilnius, Lithuania

A. Džiugys · R. Navakas (✉)
Laboratory of Combustion Processes, Lithuanian Energy Institute, Breslaujos g. 3, 44403 Kaunas, Lithuania
e-mail: rnavakas@mail.lei.lt

1 Introduction

Particulate or granular materials present a huge class of materials widely used in chemical, pharmaceutical, food and other industries. Proper understanding of mechanical behaviour of granular materials is of major importance for both fundamental developments and industrial applications. Despite the increased interest in this topic and many years of experience, the problems still remain, since experimental investigation of granular assemblies is extremely difficult. Therefore, application of numerical simulations provides a feasible alternative to physical experiments.

The discrete element method (DEM) pioneered by Cundall [1] became recognized as a tool for simulating particulate matter after the publication of the work by Cundall and Strack [2]. The DEM concept offers the unique approach capturing various particle shapes and physical models by a discrete set of quantities. Fundamentals of DEM, as well as some particular models and important details of simulation technique, may be found in [3–16].

From the computational point of view DEM may be regarded as a computational technology for modelling the motion of contacting particles as deforming bodies. The main disadvantages of the DEM technique, in comparison with the well-known continuum methods, are related to computational capabilities which are limited by a huge number of particles and a short time interval of simulations. A lot of effort was put forward to increase computational efficiency by improving particular computational procedures. It should be emphasised that DEM is a very complex technology and besides computational efficiency there is a lot of issues to be regarded to ensure the physical reality of computations. One of these problems is to deal efficiently with non-spherical shapes and to understand their behaviour.

Representation of the particle shape is one of the key challenges of DEM simulations; however most of the investigations were limited to the simplest shapes such as circular discs in two-dimensions, as introduced in [2], or spheres in three dimensions. Diversity of real particle shapes requires the development of more sophisticated particle models beyond spherical approximation. The description of complicated non-spherical shapes is based on two quite different approaches: a single-particle approach and a multi-particle approach. Discussions on possible shapes are given by Latham and Munjiza [17], Wellman et al [18] and Krugel-Emden et al. [19]. The *single particle* approach considers a particle as a single body of complicated geometry. According to Wellman et al. [18], particle types can be classified into non-smooth (or discrete) particles containing vertices, and smooth (or continuous) described by implicit or explicit continuous functions. In the most cases, smooth particles preserve convex shapes.

Elliptical particles (ellipses and ellipsoids) are probably the most widely used non-spherical smooth shapes because various types of granular matter particles are of these shapes. According to Rothenburg and Bathurst [20], the characteristics of granular material are better represented by systems of ellipsoidal particles rather than by systems of spherical particles. Various aspects of the development of the 2D elliptical particle are presented by Ting [21,22], Ting et al. [23], Wang and Liang [24] and Džiugys and Peters [6,25]. For discussions on the development and implementation of 3D contacting ellipsoids, see Lin and Ng [26,27], Ouadfel and Rothenburg [28], Wang et al. [29], Ng [30], Donev et al. [31]. Generalization of smooth particles in terms of supperellipsoid is presented in latest works of Wellman et al. [16,18] and references therein.

In order to save computational expenditure, various simplified semi-analytical approaches were elaborated for the development of non-spherical smooth convex particles. Allen and Tildesley [3] discussed the use of spherocylinders, each of which is composed of a cylinder with hemi-spherical ends of the same radius as the main body, for molecular dynamics simulations. Applications of spherocylinders to simulate granular materials are presented by Langston et al. [32] and Pournin et al. [33]. Li et al. [34] focused on the use of sphero-disc shaped particles. There, the 3D disc particles are modelled by intersection of two spheres. Description of an ellipsoid by a four-arch (Wang et al. [29], Johnson et al. [35]) may be assigned to this category as well.

In the context of DEM, the *multi-particle* approach is basically restricted to *multi-sphere (MS) models* where a single particle is represented by a composition of the connected spheres. General approach to representation and description of rotation of axi-symmetrical non-spherical particles by rigidly connected multi-spheres is presented by Favier et al. [36] and Jensen et al. [37]. Multi-sphere particles are implemented into commercial software PFC [38] and EDEM [39].

Several reported applications of multi-sphere models, referred to as a *clump*, were already examined for different purposes and various shapes. Applications include three-particle clusters (Jensen et al. [37]), irregularly shaped railway ballast particles (Lu and McDowel [40]), agricultural axisymmetric particles with high aspect ratio (Abbaspour-Fard [41]), variously shaped clay grains (Kock and Huhn [42]), tablet-shaped particles (Song et al. [43]).

There have been several attempts to use multi-spherical particles for modelling ellipsoids. Probably, the simplest 3D model of ellipsoidal particles presented by a cluster of four identical inscribed spheres was considered by Vu-Quoc et al. [44]. The 2D model of elliptical particles composed of identical discs was studied by Emeriault and Claquin [45]. Packing of arbitrary shaped multi-sphere objects including ellipsoids with a general advancing front technique was considered by Löhner and Oñate [46].

Multi-sphere composite particle models may be classified as non-convex non-smooth particles, therefore, several distinguished features including physical effects and computational aspects should be taken into account. Consequently, the most serious issue, however, related to MS approach is that knowledge on the validity of this approach is rather scarce. It is supposed that increasing the number of sub-spheres to form an elliptical particle should yield the smooth particle in the limit. To be able to solve problems using MS particles, e.g., the one shown in Fig. 1, it is important to answer the most important questions—is it possible to describe the ellipsoidal particle by MS model, how many sub-spheres are needed for the description, or to know what differences, compared to the exact solution, may occur when a limited number of sub-spheres is used. On the other hand, with the increasing number of sub-spheres, a significant increase of computational expenses is expected.

Another significant property of MS particles is a possibility to have more than one contact point during the same collision at the same time moment, while single convex particles may have only one. The net effect of such multiple contacts is still not fully understood, and, while it is commonly recognized that behaviour of a single particle and a multi-shape particle may considerably differ, the systematic numerical studies of MS approximation are however limited. Dependence of damping of multi-particle system on number of cavities was found by Saeki [47]. Similar effects in terms of differences between smooth (binary) and rough (multiple) surface contacts are considered by Leszczyński [48]. Song et al. [43] and Krugel-Emden et al. [19] studied the single tablet shaped and spherical particles, respectively, approximated with a varying number of sub-spheres. It was concluded that differences in dynamics behaviour of a single particle and a multi-particle may be a source of errors, and further stud-

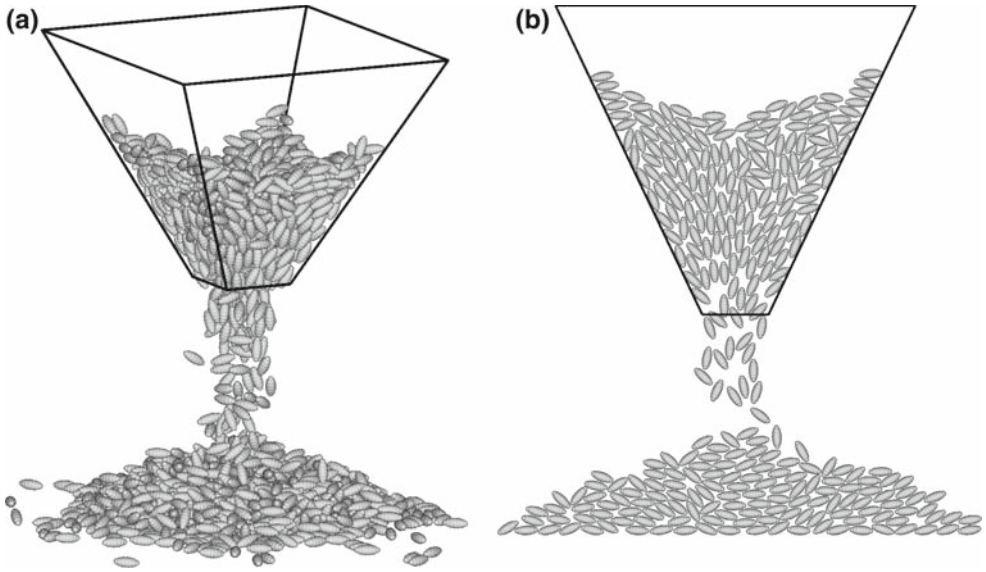

Fig. 1 Piling via the hopper discharge by multi-sphere ellipsoids: **a** 3D model, **b** 2D approach

ies are required to determine optimal approximations and to check the multi-sphere method for its capabilities to simulate larger particle assemblies.

It should be clear; however, that any precise mathematical description of a smooth particle provides only an exceptional case that does not necessarily match the real particles that are characterized, as a rule, by irregular shapes. Detailed advanced experimental measurements allow to quantify particle shapes by applying various indicators. Shukumaran and Ashmaway [49] suggested normalized shape and angularity factors to evaluate deviation of the real shape from the circular shape. Robinson and Friedman [50] used alternative shape factors, sphericity and circularity. Roughness as an indicator of particle shape is applied for interpretation of experimental results and MS models (Krugel-Emden et al. [19]). Angularity as microscopic characteristic of polygonal particles is used by Nouguier-Lehon et al. [51]. Roughness and sphericity were also used to characterise sedimental particles by Kock and Huhn [42]. Influence of various shapes factors are studied experimentally [42,47,48]. DEM analysis of many particle systems is basically restricted to two-dimensional non-convex MS particles [42] or polygons [51].

It could be stated; however, that adequacy of the MS approximation for other shapes by applying DEM is still problematic and requires further investigation. This paper addresses the multi-sphere model of ellipsoids and its application. The approximation of smooth ellipsoidal particles by MS particle model is demonstrated by solving a 2D piling problem by 3D particles. Since a purely 3D model of a MS particle is used for the present investigation, conclusions could be applicable to 3D problems.

The first purpose of this paper is to clarify the adequacy of approximation and the effort required for the description of the smooth ellipsoid and, second, to show that the performed study may serve as a basis for future applications of the 3D MS particles for problems with rough ellipsoidal shape.

The paper is arranged as follows. The models of multi-sphere ellipsoidal particle are briefly described in Sect. 2. The DEM methodology with particular emphasis on description of motion and inter-particle forces is presented in Sect. 3. The solution of a piling problem and numerical results with discussion on adequacy of MS approximation are presented in Sect. 4. Computational efficiency determined by solving benchmark tests is considered in Sect. 5, while conclusions are given in Sect. 6.

2 Multi-sphere ellipsoidal particle

MS-model presents a technique for defining ellipsoid geometry by an arbitrary number of inscribed spheres. The three-dimensional ellipsoid may be described in the local particle fixed Cartesian coordinates $Oxyz$ (Fig. 2). The local coordinate system is attached to the mass centre and rigidly connected to the particle. Assuming axial symmetry with respect to axis Ox, the geometry of the ellipsoidal particle i is defined by the major and minor half-lengths of the principal axes a and b, respectively; more precisely, by aspect ratio $s = a/b$. Hereafter, subscript i will be omitted for the sake of simplicity. The position of an arbitrary point within the particle may be presented by vector $\boldsymbol{x} = \{x, y, z\}^T$.

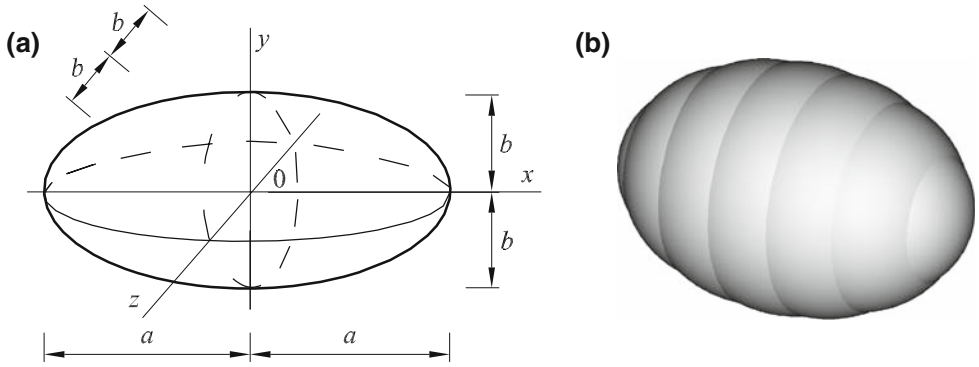

Fig. 2 Axi-symmetric three-dimensional ellipsoid: **a** geometry, **b** MS model

Consequently, the ellipsoid equation reads as follows:

$$f\,(x, y, z) = \left(\frac{x}{a}\right)^2 + \left(\frac{y}{b}\right)^2 + \left(\frac{z}{b}\right)^2 - 1 = 0. \tag{1}$$

In order to solve the equations of motion, a position of the gravity centre, the mass, and the principal mass moments of inertia should be defined for the particle under consideration. The gravity centre of an ellipsoid coincides with its geometrical centre. The cross-sectional area A in the plane Oxy and the volume V of an ellipsoid are determined by

$$A_{ell} = \pi ab, \quad V_{ell} = \frac{4}{3}\pi ab^2, \tag{2}$$

According to the MS model, the ellipsoid (Fig. 2b) is composed of N spheres, or sub-spheres, where N is an odd number. Sub-spheres are rigidly fixed with respect to each other and are located on the symmetry axis Ox.

The construction of the MS particle may be considered in two dimensions and is limited to the half of the ellipsoid along a positive semi-axis $0 \le x \le a$ (Fig. 3a). This region is occupied by n sub-spheres, where $N = 2n + 1$. Sub-spheres are denoted by subscript k, where $k = 0$ for the central largest sub-sphere, while the remaining sub-spheres are denoted as $k = 1, 2, \ldots, n$. Each of the sub-spheres is characterized by its centre coordinate x_k, variable inter-sphere distance d_k and variable radius R_k. It is obvious that for the central sub-sphere $x_0 = 0$, $R_0 = R_{\max} = b$. The length of the inter-sphere segment is $d_k = x_k - x_{k-1}$. Considering the above relation, the sub-sphere centre may be characterized in terms of segment lengths d_k as $x_k = \sum_{j=1}^{k} d_j$.

Sub-spheres present the inscribed approximation of the ellipsoid; therefore, each of sub-spheres remains tangent to the ellipsoidal surface (Fig. 3a). At the point of tangency denoted hereafter by t_k, ordinates of the ellipse $y_{\text{ell}}(x_{tk})$ defined by (1) and the sub-sphere k defined by $(x_{tk} - x_k)^2 + y_{tk} = R_k^2$, as well as their first derivatives, should be equal. Differentiation of surface equations and elimination of $\mathrm{d}y/\mathrm{d}x$ yields the tangent point position t_k as

$$x_{tk} = x_k \frac{a^2}{a^2 - b^2}. \tag{3}$$

Sequential elimination of y and inserting the position (3) yields the radius of the inscribed sub-sphere R_k as follows:

$$R_k^2 = \frac{b^2}{a^2 - b^2}\left(a^2 - b^2 - x_k^2\right). \tag{4}$$

It should be noted that the tangent point should remain within the ellipse, therefore, the expressions (3) and (4) are valid upon the condition $x_{tk} \le a$. The limit case $x_{tk} = a$ indicates the location x_n of the smallest sub-sphere n and its radius R_n in this way:

$$x_n = a - R_n,\ R_n = R_{\min} = \frac{b^2}{a}. \tag{5}$$

By assembling the sub-spheres in the ellipsoid, we obtain, in fact, a combination of n spherical segments with their centres aligned along the positive semi-axis of the ellipsoid. It is necessary that the sub-spheres overlap, therefore, the total length of the segment is as follows:

$$\sum_{k=1}^{n} d_k = a - R_{\min}. \tag{6}$$

If this condition is not fulfilled, which is possible in the case of a small number of sub-spheres and higher aspect ratios, it is necessary to increase N.

Positioning of the inner sub-spheres is based on the assumption that inter-sphere distances vary proportionally to the ellipsoid shape, therefore

$$\frac{y_{k-1}\,(x_{k-1})}{d_k} = \frac{y_k\,(x_k)}{d_{k+1}}$$

From here, the recurrent relationship for distances between the neighbouring sub-spheres may be established in the following way

$$d_{k+1} = d_k \frac{y_k\,(x_k)}{y_{k-1}\,(x_{k-1})}. \tag{7}$$

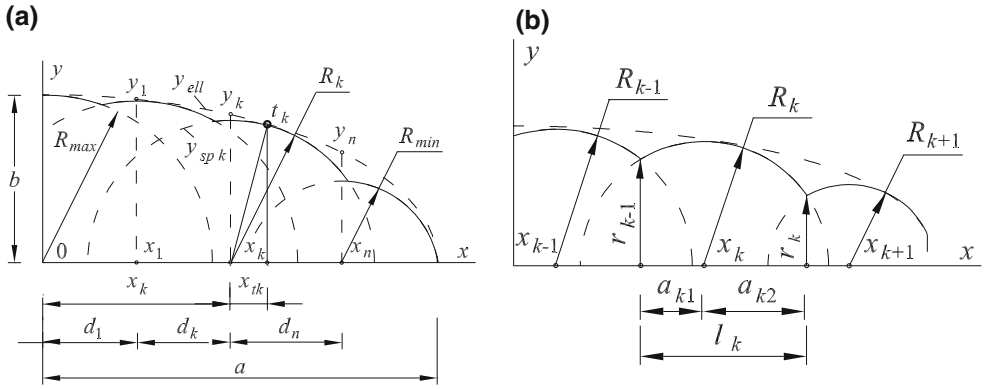

Fig. 3 Multi-sphere model of ellipsoid: **a** section geometry; **b** cut-off-spheres

Here, a position of the point on the surface of the ellipse $y_k\,(x_k)$ is obtained by substituting the coordinates of the sphere centre by solving Eq. (1). It is obvious that, for the central sub-sphere, $y_0 = b$. Substituting expressions (7) into Eq. (6) yields a non-linear equation with respect to the length of the first segment d_1:

$$d_1 + \sum_{k=2}^{n} d_k\,(d_1) = a - R_{\min}. \tag{8}$$

After solving this equation numerically, the lengths of the remaining segments d_k $(k = 2, \ldots, n)$ are obtained by sequential application of (7). The final geometry of the MS particle is defined by calculating the sub-sphere overlap and composition of cut-off-spheres as illustrated in Fig. 3b. Particular geometry of the cut-off spheres is defined by segment lengths a_k and a_{k+1} and overlap radii r_k and r_{k+1} of kth spherical segment.

The section area and volume of the MS particle are defined as the sum of areas and volumes of N sub-sphere segments, respectively. Consequently, the area A_k and volume V_k of the cut-off sub-sphere $k(k = 1, \ldots, n-1)$ is defined as the area and the volume of the spherical segment, while for the end sub-sphere $k = n$, they are defined as those for the spherical cap, respectively:

$$A_k = R_k^2\left(\pi - \cos^{-1}\left(\frac{a_{k1}}{R_k}\right) - \cos^{-1}\left(\frac{a_{k2}}{R_k}\right)\right) + a_{k1}r_{k-1} + a_{k2}r_k, \tag{9}$$

$$V_k = \frac{1}{6}\pi l_k\left(3r_{k-1}^2 + 3r_k^2 + l_k^2\right). \tag{10}$$

The above relations (1–12) serve as the basis for the description of MS ellipsoidal particle implemented in DEM.

Four ellipsoidal particles with various aspect ratios $s = 1.5$, $s = 2.35$, $s = 5.0$ and $s = 10.0$ approximated by different numbers of sub-spheres are studied. The side view of the MS ellipsoids is presented in Fig. 4.

The purely geometric effect of the MS approximation in two dimensions may be evaluated by a relative cross-section area which is the ratio of the approximated MS cross-section area A_{MS} to the one of smooth ellipse A_{ell}. Another microscopic characteristic is the relative perimeter of cross-section defined in a similar way as the ratio perimeter of MS cross-section area P_{MS} to the one of smooth ellipse.

The variation of the relative cross-sectional area upon the number of sub-spheres N is presented in Fig. 5a, while the variation of the relative perimeter is shown in Fig. 5b. These graphs indicate the effect of purely geometric microscopic approximation that can influence the macroscopic behaviour. They provide a rough idea about the required number of sub-spheres considerably affected by the aspect ratio. For the particles with aspects ratio $s = 2.35$, 1% tolerance of the section area will be achieved with 13 spheres, while the equivalent volume tolerance will be achieved with 15 spheres.

3 DEM methodology

The DEM methodology considered in this paper is aimed at simulating the dynamic behaviour of non-cohesive frictional visco-elastic dry granular matter. From the modelling point of view, granular matter is a system of the finite number of deformable bodies with the given geometry and material properties. As the particles move, they impact each other and undergo deformations. Evaluation of particles motion and contacts calculation is the most important items of the DEM methodology.

3.1 Motion of the particle

The motion of the particle as a rigid body described in the framework of classical mechanics naturally consists of two types of motion. Although a description of translational motion is independent of the particle shape, this is not the case for rotational motion. Generally, the free body motion

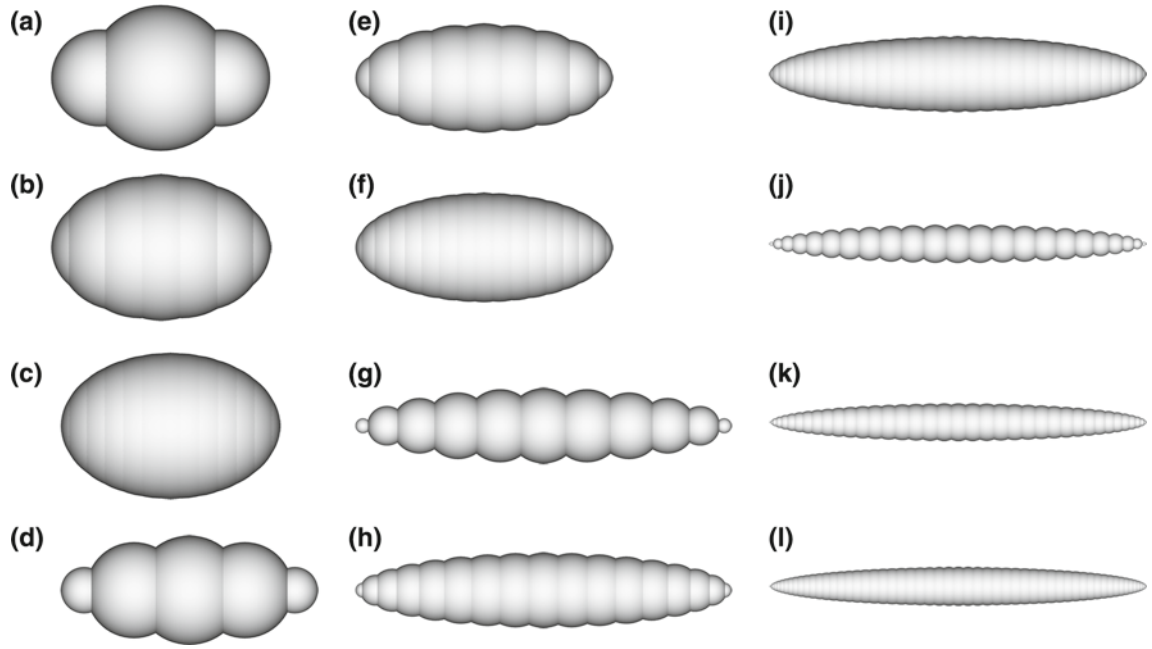

Fig. 4 Sectional geometry of multi-sphere model for ellipsoids with various aspect ratios s and number of sub-spheres N: **a** s=1.5, N=3, **b** s=1.5, N=7, **c** s=1.5, N=13, **d** s=2.35, N=5, **e** s=2.35, N=9, **f** s=2.35, N=17, **g** s=5.0, N=11, **h** s=5.0, N=17, **i** s=5.0, N=33, **j** s=10, N=23, **k** s=10, N=37, **l** s=10, N=55

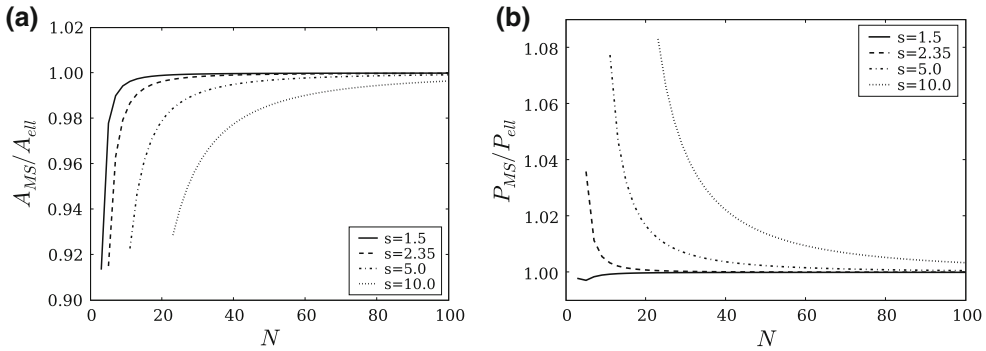

Fig. 5 Variation of the relative cross section area **(a)** and perimeter **(b)** depending on the number of sub-spheres for various aspect ratios

framework used in the multi-body dynamics may be applied to describe the particle rotation (see [52]). The motion may be described in the global (space-fixed) and local (particle-fixed) Cartesian reference frame. A position of an arbitrary point in the global coordinates is defined by its position vector $X = \{X_1, X_2, X_3\}^T$. The translational behaviour of arbitrary particle i is characterized by a small number of global parameters: positions X_i, velocities $\dot{X}_i$ and accelerations $\ddot{X}_i$ of the mass centre, as well as the resultant force vector $\boldsymbol{F}_i$ acting on the particle. The motion of particle i obeys the Newton's second law and is formulated for the mass centre of the particle as

$$m_i \ddot{X}_i (t) = F_i (t) . \tag{11}$$

The equations describing the rotational motion, or Euler equations, are derived by assuming conservation of angular momentum for particle i and may be considered in the same way. The rotation is governed by three independent rotational degrees of freedom defined by vector $\theta_i (t) = \{\theta_{i1} (t), \theta_{i2} (t), \theta_{i3} (t)\}^T$. Contrary to translational motion, definition of rotational degrees of freedom is not unique, and there exist different possibilities of their definition. Conventionally, the rotational degrees of freedom are related to rotation angles. In the most useful case of Euler angles ϕ, θ, ψ, vector of angular variables reads as $\theta_i (t) = \{\varphi_i (t), \theta_i (t), \psi_i (t)\}^T$. It would be desirable, however, to deal with explicitly defined rotational variables of the particle. Angular velocities of the particle defined by vector $w_i (t) = \{w_{i1}, w_{i2}, w_{i3}\}^T$ may be related to $\theta_i (t)$ by nonlinear rotational Jacobi matrix

$$[\mathrm{H}_{Ri} (\theta_i, t)] : \quad w_i (t) = [H_{Ri} (\theta_i, t)] \left[\dot{\theta}_i (t)\right] . \tag{12}$$

Finally, taking into account the properties of the inertia tensor of ellipsoid, Euler equations read as

$$\begin{aligned} &I_{\min}\dot{w}_i = T_{i1} \\ &I_{\max}\dot{w}_{i2} - (I_{\max} - I_{\min})\, w_{i1} w_{i3} = T_{i2}\,, \\ &I_{\max}\dot{w}_{i3} + (I_{\max} - I_{\min})\, w_{i2} w_{i1} = T_{i3} \end{aligned} \tag{13}$$

where $T_i = \{T_{i1}, T_{i2}, T_{i3}\}^T$ is vector of the external torque with respect to the particle mass centre. Inertia properties are defined by two principal moments $I_{\min} = I_1$ and $I_{\max} = I_2 = I_3$.

A detailed expression of equations of motion (13) depends on a particular choice of rotation variables. In order to avoid degeneracy of angular variables, the method of quaternions [3,6] was applied hereafter.

The numerical solutions of differential equations (11-13) for each particle i at the time $t + \Delta t$ (where Δt is the time step) is performed by using 5th order Gear's predictor-corrector [3,6] scheme featuring better tolerance [53].

3.2 Inter-particle contact

Generally, the evaluation of a binary contact comprises several tasks such as contact detection, calculation of the contact point coordinates, geometry of the overlap, normal and tangential kinematical vectors and, finally, inter-particle forces. It is the most CPU time consuming procedure; therefore, considerable effort is given to develop efficient algorithms.

Probably the most comprehensive performance study of the two mostly used tree-based and cell-based contact detection algorithms is given by Han et al. [15]. This as well as majority other studies are restricted by various limitations, therefore, universal evaluation still remains problematic. There is a large scatter in reported values of relative time spent for contact detection. Depending on various particular factors such as static configuration, specified domain and particle geometry, etc., it may comprise from 5% [15] up to 70% [54]. Consideration of contact point detection depends on each particular shape. Modelling of contact detection for smooth particles such as ellipsoids and superellipsoids is generally possible by iteratively solving sets of non-linear equations [6,18]. Contact detection for discrete particles such as convex polyhedral is related to increased amount of data related to irregular discrete geometry and particular interaction mechanisms [54].

Detection of multiple contacts for non-convex particles is even more complicated while a specific approach would be desired. Application of level set technique is elaborated for smooth contacts [55,56] or fast multipole method or ray crossing technique [57] for non-convex polygons.

The main advantage of the MS method is that contact detection and force calculation can be based on the simple algorithms valid for discs or spheres. Therefore, for the contact search we used cell-based method, which was extensively used in other codes and applications [58,59].

Description of inter-particle contact required for evaluation of contact forces $\boldsymbol{F}_i$ and torques $\boldsymbol{T}_i$ in equations (11) and (13) presents an important part of the DEM methodology. This methodology will be further illustrated by considering a general approach. Contact geometry for elliptical particles is illustrated in Fig. 6a, while that for spherical particles is given in Fig. 6b.

Let us consider two contacting particles i and j with their radii-vectors X_i and X_j, the centres of gravity O_i and O_j, the translational velocities $v_i \equiv \dot{X}_i$ and $v_j \equiv \dot{X}_j$ and the rotational velocities w_i and w_j. Vector $\boldsymbol{x}_{ij}$ of the relative position points from the centre of gravity of particle i to that of particle j

$$x_{ij} = X_i - X_j. \tag{14}$$

The particle deformation due to collision is assumed to be approximated by the overlap area of the particles. The contact point C_{ij} is defined to be in the centre of the overlap area with the position vector $\boldsymbol{X}_{cij}$. The depth of the overlap is h_{ij}, provided that it is much smaller than the particle size.

The vectors at the particle contact point can be separated into the components normal and tangential to the contact surface denoted by the superscripts n and t, respectively. The normal direction of the contact surface is defined by the unit vector $\boldsymbol{n}_{ij}$ extending through the centre of the overlap area. The unit vector $\boldsymbol{t}_{ij}$ of the tangential contact direction is perpendicular to $\boldsymbol{n}_{ij}$.

The vectors $\boldsymbol{d}_{cij}$ and $\boldsymbol{d}_{cji}$ point from the centres of the particles to the contact point C_{ij}

$$d_{cij} = X_{cij} - X_i, d_{cji} = X_{cij} - X_j. \tag{15}$$

The relative velocity of the contact point is defined as

$$v_{ij} = v_{cij} - v_{cji}, \tag{16}$$

where

$$v_{cij} = v_i + w_i \times d_{cij}, \quad v_{cji} = v_j + w_j \times d_{cji} \tag{17}$$

are the velocities of the particles i and j at the contact point.

For a contact with partial slip, the particles may slip relatively to each other along the distance δ_{ij}^t in the tangential direction:

$$\delta_{ij}^t = \left| \int v_{ij}^t\,(t)\, dt \right|. \tag{18}$$

In this case, δ_{ij}^t is allowed to increase until the tangential force exceeds the limit imposed by static friction.

Formally, the inter-particle geometry and kinematics described by (14)–(18) do not depend on the particle shape. For the spherical particles, the position of the contact point C_{ij} is on the line connecting the particle centres. Therefore, the normal contact direction $\boldsymbol{n}_{ij}$ always coincides with this

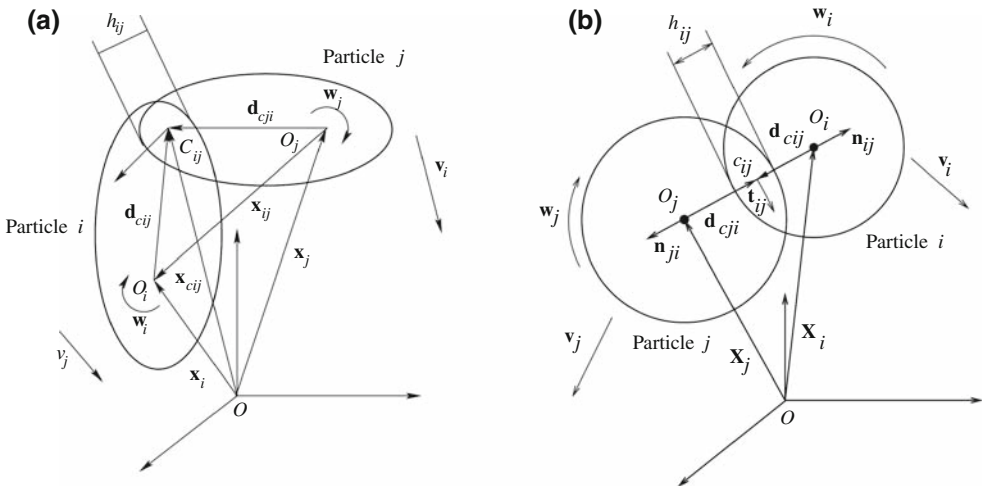

Fig. 6 Geometry of the contact of elliptical **(a)** and spherical **(b)** particles

line, while the overlap size h_{ij} is defined by considering the distance between the centres of the spheres.

Another important geometrical parameter of the contact is the reduced radius R_{ij} of the particles i and j at the contact point. Generally, it is defined as follows:

$$R_{ij} = \frac{1}{2\sqrt{AB}}, \tag{19}$$

where A and B are related to the radii of the particle shape curvatures.

For *spherical particles* in the contact with the radii R_i and R_j, we have:

$$R_{ij} = \frac{R_i R_j}{R_i + R_j}. \tag{20}$$

The details for explicit evaluation of the contact parameters, such as contact point C_{ij}, the depth of the overlap h_{ij}, the reduced radius R_{ij}, etc. for spherical and elliptical particles may be found in Džiugys and Peters [6,25].

The analysis of elliptical particles exhibits, however, considerable differences. Various analytical methods of contact detection for two- and three- dimensional elliptical particles are considered in [6].

For the present simulation, the particle shapes were defined as rotation ellipsoids ($a > b = c$) with the main semi-axis a lying on xy plane. As a result, the overlaps of the 3D particle shapes may be evaluated as overlaps of the 2D ellipses which are projections of ellipsoidal shapes on xy plane with the same values of semi-axes a and b. Therefore, methods for evaluation of the overlap between two-dimensional ellipses are applicable for the evaluation of contacts between three-dimensional ellipsoids in the present simulation. We used an iterative method developed by Džiugys and Peters [25].

3.3 Particle forces

In the framework of current investigation, force vector $\boldsymbol{F}_i$ in (11) and torque $\boldsymbol{T}_i$ in (13) present the sum of gravity and contact forces and torques, acting on the particle i, respectively:

$$F_i = F_{i,contact} + F_{i,gravity} = \sum_{j=1}^{K_{ci}} F_{ij} + m_i g, \tag{21}$$

$$T_i = T_{i,contact} = \sum_{j=1}^{K_{ci}} d_{cij} \times F_{ij}. \tag{22}$$

where $\boldsymbol{g}$ is vector of gravity acceleration, while j ($j = 1, \ldots, K_{cj}$) indicates contacting neighbour particles while K_{ci} presents a number of contact points for particle i, including contacts with the boundary.

The force (21) between two particles may be decomposed into normal and tangential components $F_{ij} = F_{ij}^n + F_{ij}^t$. The presented visco-elastic inter-particle contact model depicted in Fig. 7 includes a combination of elasticity, damping and friction force effects. Physical elasticity properties of particle i are defined by the elastic modulus E of the particle material, Poisson's ratio ν and shear modulus G. Inter-particle contact is defined by stiffness coefficients k_{ij}^n and k_{ij}^t, damping coefficients η^n and η^t and dynamic friction coefficient μ.

When overlap parameters are known, contact forces acting between two particles may be evaluated explicitly. For Hertz contact model, the forces are expressed as

$$F_{ij}^n = \frac{2}{3} \cdot \frac{E}{(1-\nu^2)} \sqrt{R_{ij} h_{ij}^3} n_{ij} - \eta^n m_{ij} v_{ij}^n, \tag{23}$$

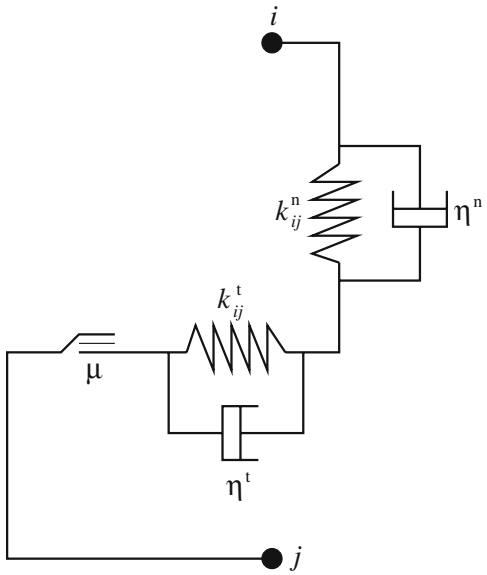

Fig. 7 Inter-particle contact model and its parameters

$$F_{ij}^{t}=-t_{ij}\,\min\left(\left|-\frac{8}{3}\cdot\frac{G\sqrt{R_{ij}h_{ij}}}{(2-\nu)}\delta^{t}{}_{ij}-\eta^{t}m_{ij}v_{ij}^{t}\right|,\mu\left|F_{ij}^{n}\right|\right), \tag{24}$$

where $m_{ij}=\frac{m_i m_j}{m_i+m_j}$ is reduced mass; v_{ij}^{n} and v_{ij}^{t} are normal and tangential components of relative velocity of the colliding particles.

3.4 Evaluation of contact parameters for multi-sphere ellipsoids

Application of basic expressions (21)–(22) to the evaluation of contact forces and torques for multi-multi-particle ellipsoids are somewhat different from the single-particle case. Generally, the contact detection of MS particles (Favier et al., [36]) uses the simplest methodology of contacting spheres. However, two distinct features should be taken into account and, therefore, the above expressions have to be slightly modified.

Firstly, not only a single conventional contact but multiple contacts between the interacting ellipsoids may occur. Consequently, the contacting points for each constituent sub-sphere $ij\,(j=1,K)$ of particle i is indicated by $k(k=1,N_{cij})$. The sum of $\sum_j N_{cij}$ may include multiple contacts.

Secondly, the directions of contact forces obtained by (23)–(24) for contacting sub-spheres are defined with respect to separate sphere centres characterised by vectors $\boldsymbol{x}_{ik}$ but not with respect to the ellipsoid centre $\boldsymbol{X}_i$. Consequently, the sphere torques $\boldsymbol{T}_{ijk}$ should be transferred to the centre of the ellipsoid.

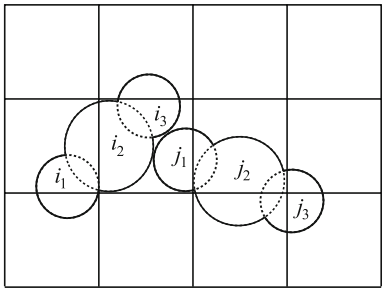

Fig. 8 Multi-sphere particles in the neighbouring cells

Finally, the resultant contact force and torque is defined by the following expressions:

$$F_{i,contact}=\sum_{j=1}^{K_{ci}}\sum_{k=1}^{N_{cij}}F_{ijk},$$

$$T_{i,contact}=\sum_{j=1}^{K_{ci}}\sum_{k=1}^{N_{cij}}\left(x_{ik}+d_{cijk}\right)\times F_{ijk}, \tag{25}$$

where $\boldsymbol{F}_{ijk}$ is the resulting contact force acting upon the sub-sphere k.

To eliminate the effect of multiple contacts correction of forces (25) is suggested in [19]. In our case, effect multiple contacts is exposed below by comparison with smooth ellipsoid.

In order to evaluate forces F_i according to equation (25) acting on the particles all contacts between the particles and their neighbours must be detected. In order to reduce the number of all particle pair combinations, a cell based algorithm is used. A three-dimensional domain of the granular media is divided into cubic cells of the size equal to the diameter of the largest sub-sphere (Fig. 8). The contacts are checked between the sub-spheres of particles in the neighbouring cells.

The developed 3D multi-sphere particle was implemented into the original code DEMMAT [60,61] and the 3D rotational ellipsoid in the plane was implemented into the code DEMCPP [62].

4 Application to the piling problem

Generally, investigation of a piling problem provides fundamentals for understanding the microscopic mechanics of granular media and the particle models. In particular, the piling technique is used for evaluating the angle of repose as one of the characteristics of granular material. Recently, the piling problem has been extensively explored in DEM simulations of the experimental data. The review of the earliest contributions based on the computer simulations is given by Herrmann and Luding [4] and references therein. The current situation in experiments and numerical simulations with

spherical particles is presented by Li et al. [63]. Simulation of piling process using non-spherical composite particles composed of five spheres is considered by Buchholtz and Pöschel [64], while different shapes were considered by Robinson and Friedman [50].

4.1 Description of the piling problem and basic data

The two-dimensional one-side piling of three-dimensional ellipsoidal particles was simulated by the DEM to illustrate the use of MS approach in approximation of the smooth ellipsoidal particles. The limitation to a two-dimensional problem was motivated by the simplicity and better transparency of simulation results in order to discover the essential properties of the MS model.

The particles are sequentially dropped and fall down under the action of gravity into the domain below bounded by the left vertical and bottom walls (Fig. 9a). The vertical wall on the one side provides the pile symmetry axis, restricting the particle motion, while the opposite side remains open, allowing the particles to fall off the pile and to form the pile slope. The particles are dropped from the fixed height $y_0 = 150$ mm above the bottom plane. In order to ensure sufficient randomness, the horizontal positioning of an individual particle centre is related to the largest particle size a, varying randomly in the range between $x_1 = a + 10^{-5}$ mm and $x_2 = x_1 + 0.1$ mm. Initially, the particles were oriented in the plane, while the initial orientation angle θ_0 was introduced randomly in the range between $-\pi$ and π. The particles are dropped at a constant rate, i.e. at equal time intervals $\Delta t_{\text{gen}} = 0.04$ s. This time interval ensures the contactless motion of the falling particles.

A set consisting of $K = 1{,}000$ mono-sized 3D ellipsoidal particles was used for simulation of a piling problem. The size of the ellipsoid is defined by two values of semi-axis, $a = 2.7$ mm and $b = c = 1.15$ mm, as shown in Fig. 2a, while its shape is defined by the aspect ratio $s = 2.35$.

The particle properties are summarised in Table 1. Two principle moments of inertia of the particle obtained using the prescribed mass m and formulas for ellipsoids were used in all our simulations independently on the number of subspheres. Modulus of elasticity E is similar to that of the rice grains with moisture content of 20% [65].

4.2 Simulation and numerical results

Two kinds of numerical simulations were performed which were based, first, on using smooth ellipsoidal particles, and, second, on using MS ellipsoidal particles. Simulations based on using smooth ellipsoidal particles serve as an "exact" reference and are applied to the evaluation of the MS models.

The process of dropping the particles lasted for 40 s for all the simulations, and, in order to reach the equilibrium state,

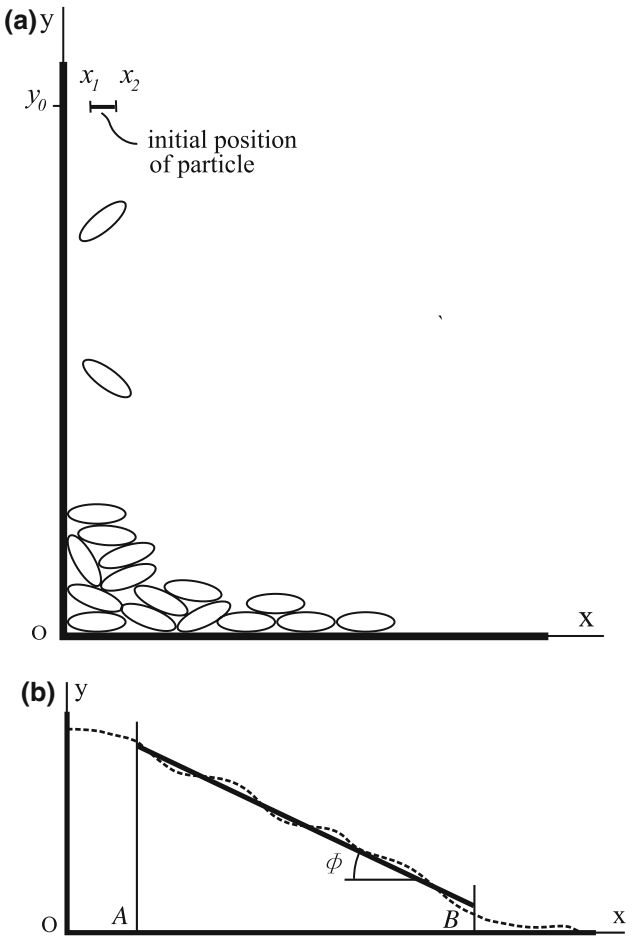

Fig. 9 A schematic view of piling: **a** dropping of particles, **b** evaluation of repose angle

Table 1 Main parameters of the particle material

Parameter	Symbol	Value
Mass, kg	m	2×10^{-5}
Maximal inertia moment, kg m^2	$I_{\max}$	3.445×10^{-11}
Minimal inertia moment, kg m^2	$I_{\min}$	1.058×10^{-11}
Elasticity modulus, Pa	E	183×10^6
Poisson's ratio	ν	0.20
Shear modulus, Pa	G	76.5×10^6
Friction coefficient	μ	0.3
Normal viscous damping coefficient, 1/s	η_n	100.0
Tangential viscous damping coefficient, 1/s	η_t	100.0

the DEM simulations were extended for the additional 10 s after the last particle was dropped. The constant time step $\Delta t = 2 \bullet 10^{-6}$ s was used in simulations.

It was previously known that a piling problem is an unstable phenomenon rather sensitive to initial random factors [4,64]. In order to capture the effect of scattering, the experi-

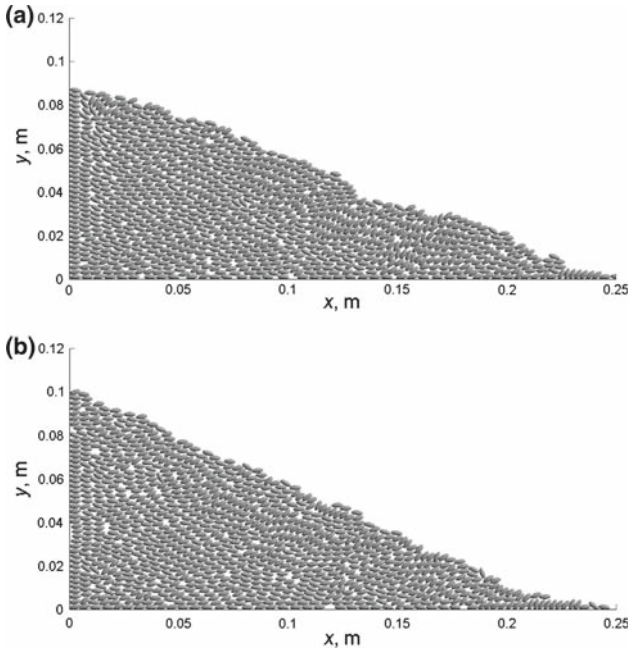

Fig. 10 Final shapes of the pile simulated by smooth elliptical particles: **a** $\Phi_{min} = 20.8^o$, **b** $\Phi_{max} = 24.4^o$

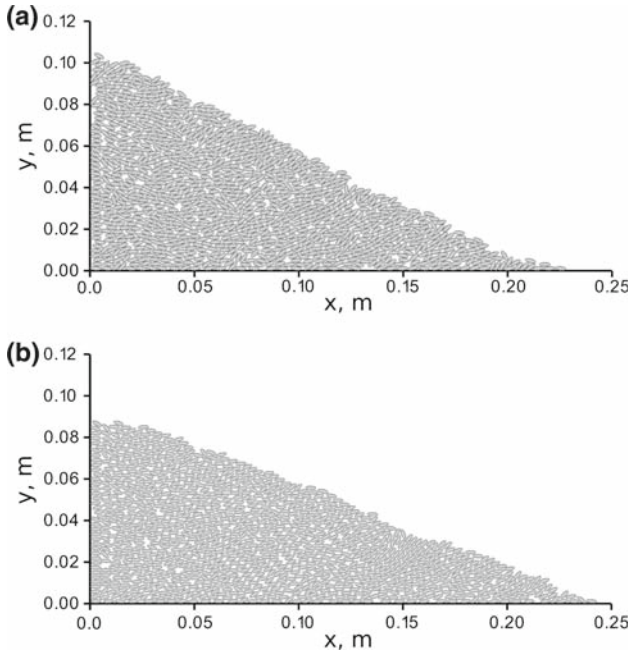

Fig. 11 Final shapes of the pile simulated by MS particles: **a** $N = 5$, $\Phi = 26.6^o$, **b** $N = 17$, $\Phi = 22.1^o$

ments were repeated 15 times for smooth ellipsoids and, due to a large amount of computations, five times for MS particles for each different number of sub-spheres. The angle of repose, porosity and coordination number were examined to evaluate the adequacy of the MS approximation.

4.2.1 Angle of repose

The earlier investigations on particle piling have shown that the profile of the pile is globally close to the straight line [64]. It was also observed that the repose angle defined as a slope may locally vary along the wedge. Moreover, a considerable difference may occur at the top and at the bottom. In order to estimate the angle of repose Φ, a surface curve was fitted to the straight line by the least squares method (Fig. 9b). To avoid the influence of the tails near the top and the bottom, only the middle segment AB of the pile was considered for the evaluation of the slope.

In the case of piling smooth ellipsoidal particles, it was found that the repose angle varied in the range from 24.4^o to 20.8^o. Finally, the average value $\Phi_{\text{av}} = 22.7^o$ of the repose angle with the average uncertainty margin $\Delta\Phi = \pm 1.8^o (\pm 8\%)$ was obtained. The resulting piles yielding the extreme values of the repose angle are shown in Fig. 10.

A series of six simulations were performed in order to investigate the approximation effects. MS particles with a constant number of sub-spheres were used in each series. MS particles consisting of 5, 7, 9, 13 and 17 sub-spheres (Fig. 4) were constructed according to Eqs. (3–8). Additionally, a particle consisting of 3 sub-spheres was constructed with the radius of the largest central sub-sphere equal to $R_{\max} = b$ and the radii of the two remaining side sub-spheres equal to $r = (a - b)/2$. Since the MS ellipsoids retain the same mass and inertia moments for all the approximations, the differences in behaviour of different MS particles depend on the shape approximation degree. The resulting piles of particles consisting of 5 and 17 sub-spheres and the obtained repose angle are presented in Fig. 11.

The entire picture of the simulation results of the repose angle Φ including both smooth ellipsoid and MS particles is shown in Fig. 12. Hereafter, the notation "**ellipse"** is used to indicate the results obtained by using a smooth ellipsoid, and the notation "**MS"** to indicate the results of the MS approximation. The repose angle obtained using a smooth particle is depicted by a constant line along with the uncertainty margins.

The results of the MS simulations for different numbers of sub-spheres are depicted by a descending curve showing a significantly larger angle of repose than that obtained for smooth particles. This curve is characterized by the uncertainty margins varying in the range from $\pm 1.39\%$ to $\pm 0.57\%$. The analysis of the average values indicates that the difference between the highest average value $\Phi = 29.1^o$ obtained for 3 sub-spheres and that of $\Phi = 23.3^o$ obtained for 17 sub-spheres comprises up to 25% drop-off.

The graph shows that only 13 and 17 sub-spheres fall within the uncertainty margin yielding 3.7 and 2.0% difference, respectively, compared to the smooth ellipsoid case.

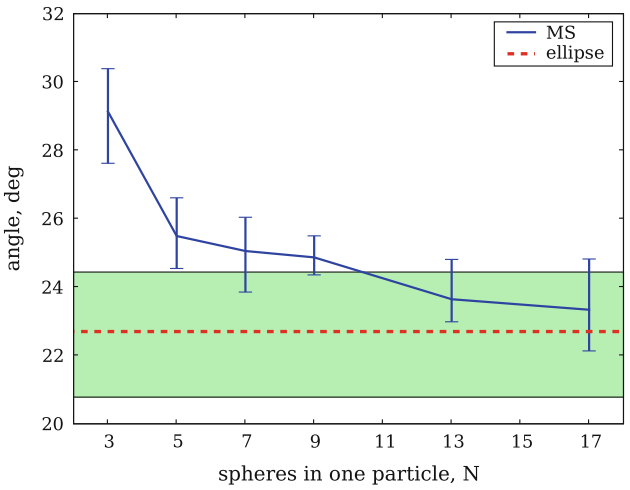

Fig. 12 Variation of repose angle for various numbers of sub-spheres

The above results indicate that generally the repose angle obtained by the MS approximation converges to that obtained from the smooth ellipse simulation. Here, the observed difference may be considered an acceptable tolerance. Consequently, a simple examination of uncertainties leads to a formal observation that 13 subspheres present a rational approximation limit sufficient to approximate a smooth particle.

Simple comparison of variations of the repose angle (Fig. 12) and relative volume or area (Fig. 5) against the number of sub-spheres indicates similar convergence tendencies for both curves. However, two specific discrepancies were also detected. First, the changes in the repose angle with the increasing number of sub-spheres exhibit a break of the tendency slope of the curve form at 9 sub-spheres and, second, they show a slower convergence rate compared to purely geometric convergence of the volume or area. The convergence of the multi-sphere model does not merely reflect only influence of the geometrical shape deviation, but probably depends on other effects.

4.2.2 Porosity

In order to better understand the complexity of the MS model, the porosity and coordination number of the resulting particle pile are examined in addition to the repose angle. The two-dimensional porosity is defined as the ratio of the area of empty space between the particles to the total area of the pile. Thorough examination of particle positions has shown that the overlap between the particles due to deformations is negligible, being of the order of 0.02%, and can be ignored. Porosity of the piling is obtained by summation of the section areas of all particles in the final state. The section areas of the MS particles can be calculated in two different ways: treating a particle either as a composition of sub-spheres, denoted as before by "**MS**", or as a smooth ellipse, denoted as "**MS ellipse**". The cross-section areas of the particles calculated according to these approaches are given by (9) or (2), respectively.

The average values and uncertainty margins of porosity are displayed in Fig. 13a. The porosity values obtained by simulating smooth elliptical particles ("**ellipse**") and by the multi-sphere approach ("**MS**") exhibit tendencies similar to those characteristic of the repose angle. The smooth particle model ("**ellipse**") yields the porosity value $p = 0.13$ with a relatively small uncertainty margin $\Delta p = \pm 4.0\%$.

The analysis of the average porosity values obtained by the purely "**MS**" approach shows fast monotonic convergences which may be explained by the difference between the cross-section areas of the MS and smooth ellipsoidal particles. The average porosity decreases from the highest value $p = 0.25$ obtained for 3 sub-spheres to $p = 0.14$ obtained for 17 sub-spheres, not reaching however the uncertainty margin of the ellipsoid case.

The **"MS ellipse"** approach yields different results. As expected, this approach shows a smaller final difference. However, another effect was identified when analysing this curve. A small number of sub-spheres, e.g. 3 or 5, allows considerable deformation-free overlap of smooth ellipses ("**MS ellipse**"). As a consequence, the overlap of the particles becomes larger, thereby reducing the empty volume. Due to this, the latter is considerably smaller than the volume given by the MS model. This effect vanishes as the number of sub-spheres increases up to $N = 7$. The above results most likely indicate the particular limit of the minimal number of sub-spheres required to be taken into account when using the MS ellipse approximation.

Qualitative illustration of both cases is presented in Fig. 14 by zooming in the final positions of the simulated particles consisting of different numbers of sub-spheres. As can be seen from the pictures, the differences between coarse and fine approximations of the particle shape result in different character of overlap, which is significant for a small number of sub-spheres.

4.2.3 Coordination number

Similar to porosity, the variation of the coordination number (average number of contacts per particle) calculated using the two approaches is examined. The conventional "**MS particle-particle**" approach defines the coordination number as the number of contacts N_{cp} between different composite particles (not between the constituent sub-spheres!) divided by the number of particles. The **"MS sphere-sphere"** approach defines the coordination number as the total number of contacts N_{cs} between the sub-spheres divided by the number of particles. The calculation of the coordination number is shown in Fig. 14b. Here, particle i is in contact with four

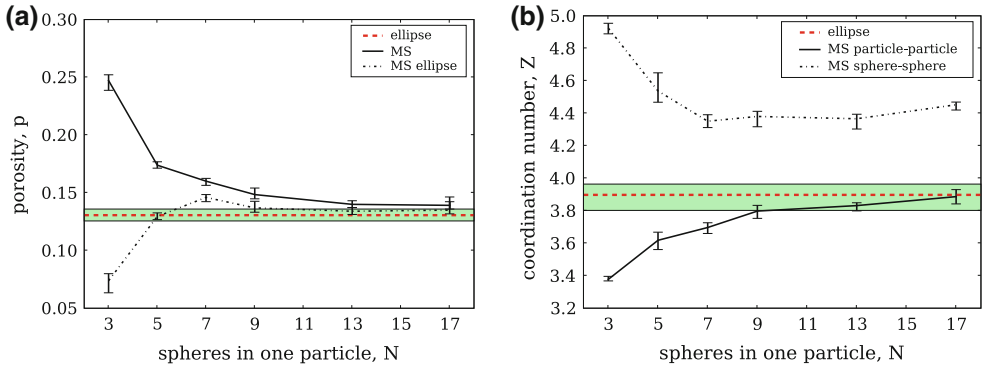

Fig. 13 Comparison of multi-sphere and elliptical models for various numbers of sub-spheres: **a** porosity: **b** coordination number

neighbouring particles, thus $N_{cp} = 4$, while the number of real contacts between the sub-spheres is $N_{cs} = 6$ as denoted in the figure.

The results obtained by using both approaches are presented in Fig. 13b. Here, it is shown that the average value of the coordination number for a smooth particle is equal to $Z_{el} = 3.90$, with the uncertainty margin of $\pm 2.5\%$. The behaviour of coordination number Z_{pp}, evaluated by "**MS particle-particle"** approach, shows practically perfect convergence of MS model with 17 sub-spheres, while nine sub-spheres are sufficient to reach the tolerance comparable to the uncertainty margin.

The results obtained for coordination number Z_{ss}, evaluated by the "**MS sphere-sphere**" approach, suggest another effect, namely, Z_{ss} increases as the number of sub-spheres increases up to $N \geq 7$ and theoretically Z_{ss} should increase up to infinity by increasing to infinity number of sub-spheres.

4.2.4 Discussion

The above results may be analyzed from other point of view regarding to deviations of MS model. The difference of MS particle shape from the smooth ellipsoidal one may be treated as a roughness of surface of MS particle, which may be quantified by several parameters. Firstly, roughness may be evaluated on the base area shape factor sf_A defined as relative deviation of cross-section area of MS particle A_{MS} from one of smooth particle A_{ell}:

$$sf_A = \frac{|A_{MS} - A_{ell}|}{A_{ell}}. \tag{26}$$

Secondly, particles roughness may be evaluated by perimeter shape factor sf_P defined as relative deviation of perimeter of MS particle shape cross-section area P_{MS} from one of smooth particle P_{ell}:

$$sf_P = \frac{|P_{MS} - P_{ell}|}{P_{ell}} \tag{27}$$

Dependency of relative of repose angle Φ_{rel} on the parameters of shape factors sf_A and sf_P (Fig. 15) might be classified in two categories: the case of small number of sub-spheres is $N \leq 9$ and the case of $N \geq 9$. On our opinion, the dependency Φ_{rel} in case of $N \leq 9$ is defined by interlocking of particles due to observed deep artificial overlap (with respect to ellipse) of MS particles. More artificial overlap due to less number of sub-spheres (minimum is 3) gives stronger interlocking, and, as a result, angle of repose is higher. Extrapolating this tendency would yield clear divergence of the MS model (in the limit of $N \to \infty$) from a smooth ellipse. This tendency changes when $N = 9$. The dependency of $N \geq 9$ case is defined by the same interlocking due to artificial overlap, but which may be treated as an additional "artificial" friction due to roughness which has tendency to converge to zero as the number of sub-spheres N tends to infinity. As a result, the angle of repose of MS particles converges to angle of repose of smooth particles, too, as the number of sub-spheres N tends to infinity.

In summary, the idea of approximating a real ellipse, even with a large number of sub-spheres, appears to be fictitious in handling realistic problems. On the other hand, it shows another perspective – the MS model could be a promising approach to handling non-smooth real particle shapes, for which a perfect ellipsoid is just an idealization.

5 Computational efficiency

The application of the developed MS model to simulation of non-spherical particles might face serious difficulties due to the increase of computational expenses. Investigation of computational efficiency of the MS ellipsoids may be separated into two tasks—estimation of computational overhead brought about by the increasing number of sub-spheres and comparing it with the computational efficiency observed in the case of elliptical particles.

The first task is performed by conducting numerical experiments. It is already known that the most time-consuming

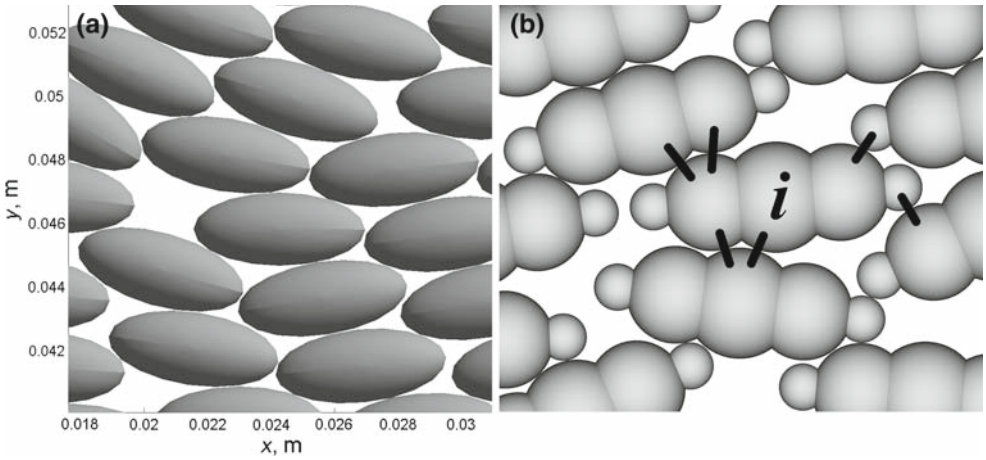

Fig. 14 Mutual positions of particles for different approximations: **a** ellipse, **b** MS particle with $N = 5$ sub-spheres

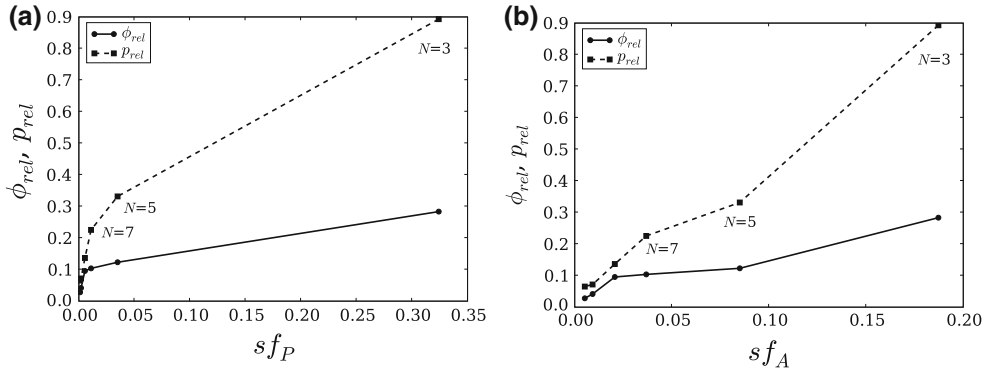

Fig. 15 Dependency of relative repose angle **(a)** and porosity **(b)** on the MS shape factors

DEM procedure is contact evaluation comprising neighbour search and calculation of contact forces. Therefore, the benchmark problem must involve the contacts between the particles continuously changing their positions.

The following procedure was chosen for the efficiency test. A rectangular box filled with 1000 particles was considered. The particles are put in motion by a one-side wall, moving towards the inside of the box (Fig. 16a). All the particles are involved into the motion and the particles' positions are changing continuously during the entire simulation period. The motion of the wall continue until $t = 0.5$ s since the start. The properties and shapes of the particles are the same as those used in the piling problem.

A series of runs with a varying number of sub-spheres were performed by applying the DEMMAT code [61] to test the efficiency of the MS approach. It is obvious that modelling of pure spherical particles is most efficient due to simplicity of the algorithm; therefore, the latter case was used as the reference. The efficiency was evaluated by means of the measured relative CPU time CPU_{rel}, i.e. the CPU time spent for the test problem divided by the CPU time spent for purely spherical particles.

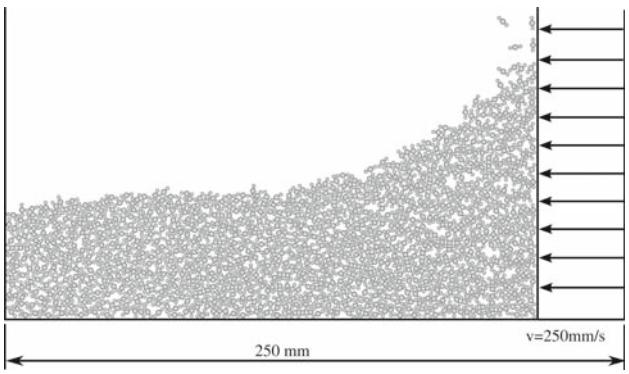

Fig. 16 Particle efficiency test by the compacting problem

A relative CPU time used for simulation of ellipsoidal particles was longer by a factor of 4.1 than that spent for simulation of spherical particles. As stated above, two-dimensional algorithm was used to resolve contacts between elliptical particles, while 3D algorithm was used for MS particles. Therefore, we are not able to directly compare computational efficiency of MS approach with that of real 3D ellipsoids. As could be seen from [6], the algorithm for 3D ellipsoids is

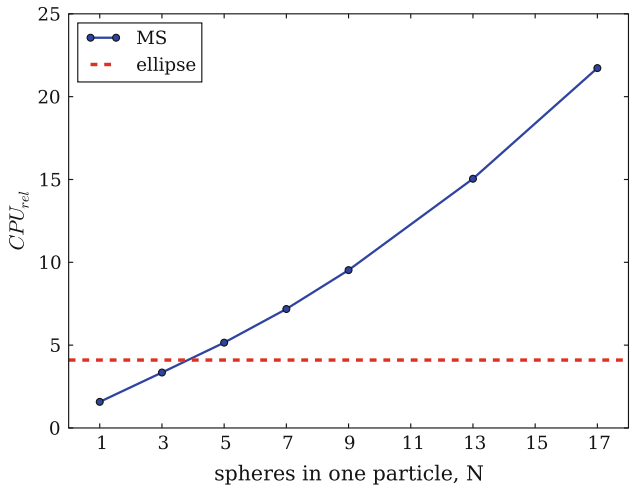

Fig. 17 Particle efficiency test: amount of the relative CPU time CPU_{rel} spent for various numbers of sub-spheres N

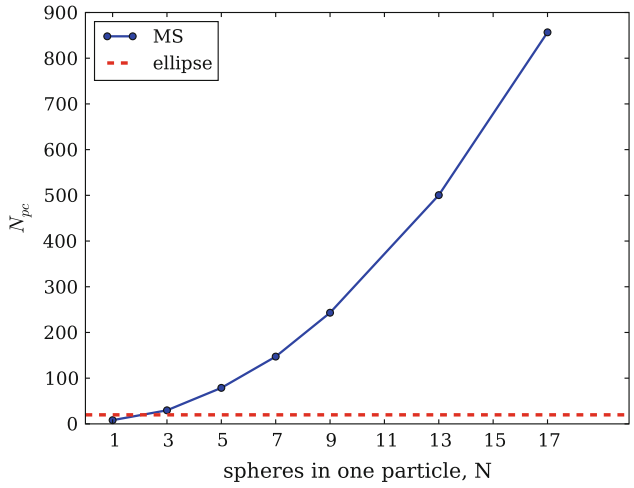

Fig. 18 Particle efficiency test: number of potential contacts N_{pc} for various numbers of sub-spheres N

more complicated than that used for 2D ellipses. Therefore, it should considerably increase the required CPU time.

The result obtained for the efficiency for MS model of various numbers of sub-spheres is presented in Fig. 17. As stated in [61], the MS algorithm used for spherical particles consisting only of one sub-sphere increases the CPU time by a factor of 1.58 compared to the case of the algorithm using purely spherical particles. As it can be seen from Fig. 17, the use of three sub-spheres for an ellipsoidal particle increases the CPU time by a factor of 3.3, while in the case of 17 sub-spheres, the increase of the CPU time is by a factor of 22, compared to the case of purely spherical particles.

Looking for reasons of such increase, the variation of number of potential contacts N_{pc} for MS particles with various numbers of sub-spheres is extracted and shown in Fig. 18 and compared with number of potential contacts for smooth ellipses which is equal to 19.8. It could be observed that computational expenses mimic number of potential contacts and this may be a reason for nonlinear increase of obtained computational time.

6 Conclusions

Adequacy of multi-sphere (MS) approximation of elliptical particles in DEM simulations was investigated. For this purposes, the multi-sphere (MS) model with the controlled variable number of sub-spheres N for the approximation of the ellipsoidal particle was developed. The MS and smooth ellipse models were investigated by two-dimensional piling of a set of three-dimensional mono-sized ellipsoids with the fixed aspect ratio $s = 2.35$. Adequacy of the MS model was evaluated by considering macroscopic parameters of granular dynamics, such as the angle of repose and porosity, as well as microscopic parameter, such as the coordination number.

The following conclusions may be drawn on the basis of the results obtained in this research:

- The piling problem is sensitive to random imperfections imposed by the piling data and numerical errors, and there is a scatter of the results. It follows that the macroscopic and microscopic parameters must be evaluated only in terms of the average values and uncertainty margins.
- In general, the adaptive multi-sphere model with increasing number of sub-spheres exhibits a clear tendency to converge to a smooth ellipsoid when applied to macroscopic parameters. The model error may be roughly evaluated in terms of shape factors.
- The increase in the number of sub-spheres yields the increase of multiple inter-particle contacts, thereby influencing the behaviour of macroscopic parameters. Therefore, the application of the MS model to microscopic analysis of particulates will require the data about the roughness of real particles.
- The observed artificial overlap of MS (compared to the case of an ellipse) influencing macroscopic behaviour may be classified into two categories: the case of a small number of sub-spheres ($N \leq 9$) may be interpreted as particles' interlocking, and the case $N \geq 9$ may be simply interpreted as a decrease of roughness when the number of sub-spheres increases.
- In summary, a multi-sphere model remains a realistic and relatively simple particle model applicable to DEM simulations of the behaviour of the real smooth and rough elliptically shaped particles. A reasonable number of sub-spheres should be chosen, however, as a compromise between the acceptable tolerance and computational expenses. More precise recommendations depend on the particular aspect ratio of the ellipsoid and detailed characterisation of particle shape.

Acknowledgments Support of "the Lithuanian State Science and Studies Foundation" under Grant No. T - 110/08 is gratefully acknowledged.

References

1. Cundall, P. A.: A computer model for simulating progressive, large scaled movements in blocky rock systems. In: Symposium of International Society of Rock Mechanics, vol. 1, II-8, Nancy (1971)
2. Cundall, P.A., Strack, O.D.L.: A discrete numerical model for granular assemblies. Geotechnique **29**, 47–65 (1979)
3. Allen, M.P., Tildesley, D.J.: Computer simulation of liquids. Oxford Science Publication, USA (1987)
4. Herrmann, H.J., Luding, S.: Modelling granular media on the computer. Contin Mech Thermodyn **10**, 189–231 (1998)
5. Luding, S., Lätzel, M., Volk, W., Diebels, S., Herrmann, H.J.: From discrete element simulations to a continuum model. Comput Methods Appl Mech Eng **191**, 21–28 (2001)
6. Džiugys, A., Peters, B.J.: An approach to simulate the motion of spherical and non-spherical fuel particles in combustion chambers. Granul Mater **3**, 231–266 (2001)
7. Pöschel, T., Schwager, T.: Computational granular dynamics, models and algorithms. Springer, Berlin (2004)
8. Munjiza, A.: The combined finite-discrete element method. Wiley, London (2004)
9. Tomas, J.: Fundamentals of cohesive powder consolidation and flow. Granul Mater **6**, 75–86 (2004)
10. Liu, W.K., Karpov, E.G., Zhang, S., Park, H.S.: An introduction to computational nanomechanics and materials. Comput Methods Appl Mech Eng **193**, 1529–1578 (2004)
11. Kruggel-Emden, H., Simsek, E., Rickelt, S., Wirtz, S., Scherer, V.: Review and extension of normal force models for the discrete element method. Powder Technol **171**, 157–173 (2007)
12. Gilabert, F. A., Roux, J.-N., Castellanos, A.: Computer simulation of model cohesive powders: influence of assembling procedure and contact laws on low consolidation states. Phys Rev E **75**, 011303 (2007)
13. Balevicius, R., Kacianauskas, R., Mroz, Z., Sielamowicz, I.: Discrete-particle investigation of friction effect in filling and unsteady/steady discharge in three-dimensional wedge-shaped hopper. Powder Technol **187**, 159–174 (2008)
14. Balevicius, R., Kacianauskas, R., Vadluga, V.: Investigation of three-dimensional granular stresses in pyramidal container after filling. Mechanika **6**, 11–16 (2008)
15. Han, K., Feng, Y.T., Owen, D.R.J.: Performance comparisons of tree-based and cell-based contact detection algorithms. Eng Comput **24**(2), 165–181 (2007)
16. Wellmann, C., Lillie, C., Wriggers, P.: Comparison of the macroscopic behavior of granular materials modeled by different constitutive equations on the microscale. Finite Elements Anal Design **44**, 259–271 (2008)
17. Latham, J.P., Munjiza, A.: The modelling of particle systems with real shapes. Phil Trans R Soc Lond Ser A Math Phys Eng Sci **362**, 1953–1972 (2004)
18. Wellmann, C., Lillie, C., Wriggers, P.: A contact detection algorithm for superellipsoids based on the common-normal concept. Eng Comput **25**, 432–442 (2008)
19. Kruggel-Emden, H., Rickelt, S., Wirtz, S., Scherer, V.: A study on the validity of the multi-sphere Discrete Element Method. Powder Technol **188**, 153–165 (2008)
20. Rothenburg, L., Bathurst, R.J.: Numerical simulation of idealized granular assemblies with plane elliptical particles. Comput Geotech **11**, 315–329 (1991)
21. Ting, J. M.: An ellipse-based micromechanical model for angular granular materials. In: Adeli, H. (ed.) Proceeding of ASCE Engineering Mechanics Conference on Mechanics, Computing in 1990 and beyond, Columbus, Part 2, pp. 1214–1218 (1991)
22. Ting, J. M.: A robust algorithm for ellipse-based discrete element modelling of granular material. Comput Geotech **13**, 175–186 (1992)
23. Ting, J.M., Khwaja, M., Meachum, L., Rowell, J.D.: An ellipse-based discrete element model for granular materials. Int J Numer Anal Methods Geomech **17**, 603–623 (1993)
24. Wang, C.-Y., Liang, V.-C.: A packing generation scheme for the granular assemblies with planar elliptical particles. Int J Numer Anal Methods Geomech **21**, 347–358 (1997)
25. Džiugys, A., Peters, B.: A new approach to detect the contact of two-dimensional elliptical particles. Int J Numer Anal Methods Geomech **25**, 1487–1500 (2001)
26. Lin, X., Ng, T.-T.: Contact detection algorithms for three-dimensional ellipsoids in discrete element modelling. Int J Numer Anal Methods Geomech **19**, 653–659 (1995)
27. Lin, X., Ng, T.-T.: A three-dimensional discrete element model using arrays of ellipsoids. Geotechnique **47**, 319–329 (1997)
28. Ouadfel, H., Rothenburg, L.: An algorithm for detecting inter-ellipsoid contacts. Comput Geotech **24**, 245–263 (1999)
29. Wang, C.-Y., Wang, C.-F., Sheng, J.: A packing generation scheme for the granular assemblies with 3D ellipsoidal particles. Int J Numer Anal Methods Geomech **23**, 815–828 (1999)
30. Ng, T.-T.: Shear strength of assemblies of ellipsoidal particles. Geotechnique **54**, 659–669 (2004)
31. Donev, A., Torquato, S., Stillinger, F.H.: Neighbour list collision-driven molecular dynamics simulation for nonspherical hard particles. II. Applications to ellipses and ellipsoids. J Comput Phys **202**, 765–793 (2005)
32. Langston, P.A., Al-Awamleh, M.A., Fraige, F.Y., Asmar, B.N.: Distinct element modelling of nonspherical frictionless particle flow. Chem Eng Sci **59**, 425–435 (2004)
33. Pournin, L., Weber, M., Tsukahara, M., Ferrez, J.A., Ramaioli, M., Liebling, T.M.: Three-dimensional distinct element simulation of spherocylinder crystallization. Granul Mater **7**, 119–126 (2005)
34. Li, J., Langston, P.A., Webb, C., Dyakowski, T.: Flow of spher-o-disc particles in rectangular hoppers—a DEM and experimental comparison in 3D. Chem Eng Sci **59**, 5917–5929 (2004)
35. Johnson, S., Williams, J.R., Cook, B.: Contact resolution algorithm for an ellipsoid approximation for discrete element modelling. Eng Comput **21**, 215–234 (2004)
36. Favier, J.F., Abbaspour-Fard, M.H., Kremmer, M., Raji, A.O.: Shape representation of axisymmetrical, non-spherical particles in discrete element simulation using multi-element model particles. Eng Comput **16**, 467–480 (1999)
37. Jensen, R.P., Bosscher, P.J., Plesha, M.E., Edil, T.B.: DEM simulation of granular media—structure interface: effects of surface roughness and particle shape. Int J Numer Anal Methods Geomech **23**(6), 531–547 (1999)
38. PFC3D, user's guide. Itasca Consulting Group, Inc., Minneapolis (1999)
39. EDEM. DEM Solutions Lt, http://www.dem-solutions.com
40. Lu, M., McDowell, G.R.: The importance of modelling ballast particle shape in the discrete element method. Granul Mater **9**, 69–80 (2006)
41. Abbaspour-Fard, M.H.: Theoretical validation of a multi-sphere, discrete element model suitable for biomaterials handling simulation. Biosyst Eng **88**, 153–161 (2004)
42. Kock, I., Huhn, K.: Influence of particle shape on the frictional strength of sediments—a numerical case study. Sedimentary Geol **196**(1–4), 217–233 (2007)
43. Song, Y.X., Turton, R., Kayihan, F.: Contact detection algorithms for DEM simulations of tablet-shaped particles. Powder Technol **161**(1), 32–40 (2006)

44. Vu-Quoc, L., Zhang, X., Walton, O.R.: A 3-D discrete-element method for dry granular flows of ellipsoidal particles. Comput Methods Appl Mech Eng **187**, 483–528 (2000)
45. Emeriault, F., Claquin, C.: Statistical homogenization for assemblies of elliptical grains: effect of the aspect ratio and particle orientation. Int J Solids Struct **41**, 5837–5849 (2004)
46. Löhner, R., Oñate, E.: A general advancing front technique for filling space with arbitrary objects. Int J Numer Math Eng **61**, 1977–1991 (2004)
47. Saeki, M.: Analytical study of multi-particle damping. J Sound Vib **281**(3–5), 1133–1144 (2005)
48. Leszczyński, J.S.: A discrete model of a two-particle contact applied to cohesive granular materials. Granul Mater **5**(2), 91–98 (2003)
49. Sukumaran, B., Ashmaway, A.K.: Influence of inherent particle characteristics on hopper flow rate. Powder Technol **138**, 46–50 (2003)
50. Robinson, D.A., Friedman, S.P.: Observations of the effects of particle shape and particle size distribution on avalanching of granular media. Phys A **311**, 97–110 (2002)
51. Nouguier-Lehon, C., Cambou, B., Vincens, E.: Influence of particle shape and angularity on the behaviour of granular materials: a numerical analysis. Int J Numer Anal Methods Geomech **27**(14), 1207–1226 (2003)
52. Schiehlen, W., Eberhard, P.: Technische dynamik. Teubner BG, Stuttgart (2004)
53. Balevičius, R., Džiugys, A., Kačianauskas, R.: Discrete element method and its application to the analysis of penetration into granular media. J Civil Eng Manag **10**(1), 3–14 (2004)
54. Nezami, E.G., Hashash, Y.M.A., Zhao, D.W., Ghaboussi, J.: Shortest link method for contact detection indiscrete element method. Int J Numer Anal Meth Geomech **30**, 783–801 (2006)
55. Tijskens, E., de Baerdemaeker, J., Ramon, H.: Strategies for contact resolution of level surfaces. Eng Comput **21**(2/3/4), 137–150 (2004)
56. Yokoi, K.: Numerical method for interaction between multiparticle and complex structures. Phys Rev **72**, 046713 (2005)
57. Muth, B., Of, G., Eberhard, P., Steinbach, O.: Collision detection for complicated polyhedra using the fast multipole method or ray crossing. Arch Appl Mech **77**, 503–521 (2007)
58. Maknickas, A., Kačeniauskas, A., Kačianauskas, R., Balevičius, R., Džiugys, A.: Parallel DEM software for simulation of granular media. Informatica **17**, 207–224 (2006)
59. Kačianauskas, R., Maknickas, A., Kačeniauskas, A., Markauskas, D., Balevičius, R.: Parallel discrete element simulation of poly-dispersed granular material. Advances Eng Softw **41**, 52–63 (2010)
60. Balevičius, R., Džiugys, A., Kačianauskas, R., Maknickas, A., Vislavičius, K.: Investigation of performance of programming approaches and languages used for numerical simulation of granular material by the discrete element method. Comput Phys Commun **175**, 404–415 (2006)
61. Markauskas, D.: Discrete element modelling of complex axi-symmetrical particle flow. Mechanika **6**, 32–38 (2006)
62. Peters, B., Džiugys, A.: Numerical simulation of the motion of granular material using object-oriented techniques. Comput Methods Appl Mech Eng **191**, 1983–2007 (2002)
63. Li, Y., Xu, Y., Thornton, C.: A comparison of discrete element simulations and experiments for "sandpiles" composed of spherical particles. Powder Technol **160**, 219–228 (2005)
64. Buchholtz, V., Pöschel, T.: Numerical investigations of the evolution of sand piles. Phys A **202**, 390–401 (1994)
65. Zhang, Q., Yang, W., Sun, Z.: Mechanical properties of sound and fissured rice kernels and their implications for rice breakage. J Food Eng **68**, 65–72 (2005)